Silver Tip Formation on Colloidal CdSe Nanorods by a Facile Phase Transfer Protocol

Tanushree Bala and Kevin M. Ryan

Abstract A facile phase transfer procedure is described for the formation of uniform silver metal tips on II–VI semiconductor nanorods. Judicious choice of a functional ligand dimethyl phenol (DMP) which binds to the semiconductor rod in the organic phase enables the transfer of metal ions from the aqueous phase and their reduction onto the nanorod. The nanorod hybrids can be assembled into perpendicularly aligned arrays by simple solvent evaporation.

Keywords CdSe nanorods · Ag tipping · Phase transfer

1 Introduction

Colloidal semiconductor nanorods synthesised by precise shape control of nanocrystals have found significant application in photovoltaics, photocatalysis and field emission devices [1–5]. These bulk applications are possible as the nanorods can be readily assembled into scalable perpendicular architectures where length dependent properties such as total absorption or emission can be independently tuned from diameter dependent properties such as band gap [2, 6–8]. Recent advances allow the formation of gold tips on the ends of the semiconductor nanorods as a sequential synthetic step in solution or by post-synthetic spin casting

T. Bala (✉)
Department of Chemistry, University of Calcutta, Kolkata, India
e-mail: tanushreebala@gmail.com

T. Bala · K. M. Ryan
Materials and Surface Science Institute, University of Limerick, Limerick, Ireland
e-mail: kevin.m.ryan@ul.ie

P. K. Giri et al. (eds.), *Advanced Nanomaterials and Nanotechnology*,
Springer Proceedings in Physics 143, DOI: 10.1007/978-3-642-34216-5_2,

on a preformed assembly [9–21]. In Au–CdSe, enhanced photocatalytic reactions are possible in solution through charge separation at the M–SC interface [6, 20, 22]. More recently, electron transfer via redox processes in a protein immobilised on metal tipped nanorod arrays was detected at a substrate demonstrating potential for sensor applications [23]. A facile route to Au tip formation has been achieved where the metal precursor either ($AuCl_3$) or more recently (AuCl) and a reducing agent are solubilized in the organic phase using surfactants. Control of the reaction time, temperature and light activation can tune the structure from double tipped (both ends) to single tip to enlarged single tip [8–14]. The organic phase reduction methods while extremely successful with Au-tipping limit the extension of the tipping protocol to other metals due to the insolubility of their metal salts in non-polar solvents. Tipping using organometallic precursors has been successful with Pt and Co although complex reaction schemes are necessary for these non-commercially available precursors [24–27]. A successful approach allowed Au and Pt tipping on rods from their water soluble salts whereby the nanorod was transferred to the aqueous phase using ligand exchange followed by reduction of the water soluble metal precursor. The tip growth is pH dependent and reaction times of up to 2 days are required [24, 28].

Here we describe a simplified protocol to yield instantaneous Ag–semiconductor nanorod hybrid structures where instead of transferring the nanorod to the aqueous phase, the metal ions are phase transferred from the aqueous to the organic phase. This we achieve by the introduction of suitable organic ligand molecules onto the surface of the nanorods possessing the bi-functionality of phase transfer and reducing capability. Tipping by this phase transfer protocol occurs at room temperature on CdSe nanorods. This method avoids the preference for the Ag ion to cation exchange with Cd forming Ag_2Se. The tipped nanorods also readily assemble into close packed super lattices from solution with the c-axis of the rod perpendicular to the substrate. The density of packing and proper assembly [29] will likely find significant application where silver metal–semiconductor hybrids are needed in high density arrays such as photovoltaics or photocatalysis [8–10].

2 Experimental Section

2.1 Synthesis of CdSe Nanorods

Materials: Cadmium oxide (CdO) was purchased from Fluka, trioctylphosphine (TOP, 90 %), trioctylphosphine oxide (TOPO, 99 %), sulfur (S), silver nitrate ($AgNO_3$), dimethyl phenol ($C_8H_{16}O$, mentioned as DMP in this paper), and toluene were purchased from Aldrich, and n-octadecylphosphonic acid (ODPA) was obtained from Poly Carbon Industries Inc. (PCI).

CdSe nanorods were synthesised with slight modifications to the published procedure [30].

2.2 Synthesis of Ag–Semiconductor Hybrids

In a typical reaction, 10 ml of 10^{-1} M DMP in toluene was injected into 15 ml of nanorod solution and the resulting mixture was sonicated before precipitating with acetone/toluene mixture. The solution was then centrifuged at 5,000 rpm for 10 min. The colorless supernatant was decanted off and the above process was repeated for 3 times. The precipitate was then re-dispersed in toluene maintaining a concentration of 0.06 mg ml^{-1}, a part of which ($\sim$5 ml) was then stirred with 5×10^{-3} M aqueous $AgNO_3$ in the presence of 5×10^{-5} M KOH solution. Aliquots of the top toluene layer were separated from the biphasic mixture at different time intervals for characterization.

2.3 Characterization Techniques

Samples were characterized using Transmission electron microscopy (JEOL 2011) at an accelerating voltage of 200 kV, UV–Vis spectroscopy (Cary-300 Bio UV–Vis spectrophotometer) operated at a resolution of 1 nm, fluorescence spectroscopy (Varian Cary Eclipse Fluorescence Spectrophotometer), X-Ray diffraction (PANalyticalX'Pert MPD Pro) using Cu Ka radiation with a 1-DX' Celerator strip detector, Fourier transform infrared spectroscopy (Perkin-Elmer-Spectrum One FTIR), X-Ray photoelectron spectroscopy (Kratos Axis 165 spectrometer). XPS high resolution spectra were taken using monochromated Al Kα radiation of an energy of 1,486.6 eV at fixed pass energy of 20 eV. For peak synthesis, a mixed Gaussian–Lorenzian function with a Shirley type background subtraction was used. Samples were flooded with low energy electrons for efficient charge neutralisation. Binding energies (BE) were determined using C 1 s at 284.8 eV as charge reference.

3 Results and Discussion

Stirring a biphasic mixture of organically soluble di-methyl phenol (DMP) with aqueous $AgNO_3$ in the presence of 5×10^{-5} M KOH resulted in the formation of Ag nanocrystals (Fig. 1a) in the organic medium (yellow colour). Nanocrystals were FCC Ag of the order of 5–10 nm in size with the density dependent on the concentration of the DMP (Fig. 1b). The introduction of CdSe nanorods that were pre-treated with 10^{-1} M DMP into the organic phase, with similar concentrations of $AgNO_3$ and KOH in the aqueous phase resulted in the nucleation of metal dots (<1 nm) onto the rod surface without additional free metal nanocrystal formation. The formation of the hybrid was schematically represented in Fig. 1c. The growth of these Ag dots was reaction time dependent with multiple grains occurring after

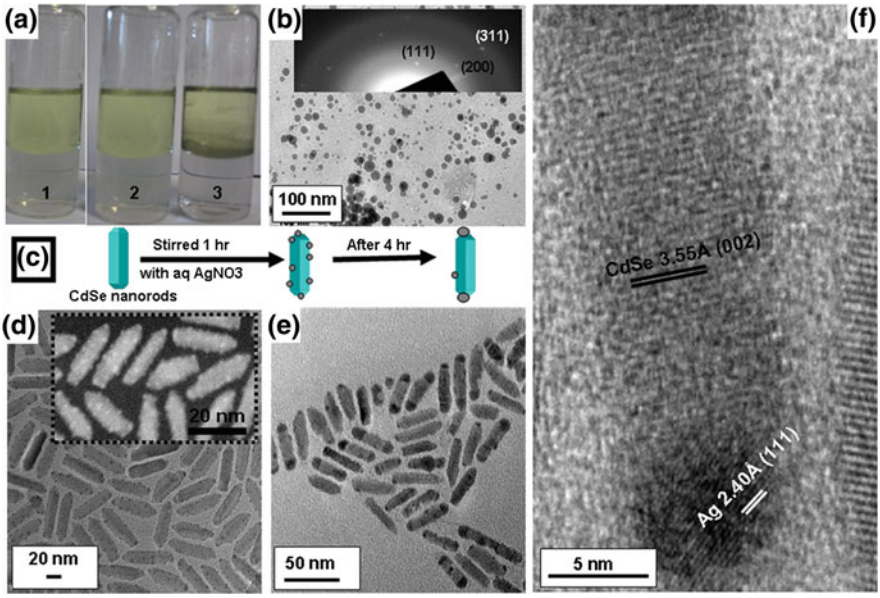

Fig. 1 **a** Photographs of the Ag nanoparticles formed using 1×10^{-4} (*photo 1*), 1×10^{-3} (*photo 2*) and 1×10^{-2} M (*photo 3*) aqueous Ag + and 10^{-2} M DMP in toluene. **b** TEM and SAED of Ag nanoparticles. **c** Schematic representation of the formation of Ag tips on bare CdSe nanorods. **d** TEM of the anisotropic growth of Ag nanoparticles all over the surface of the nanorods at t = 1 h. *The inset* shows STEM of Ag tipped CdSe nanorods. **e** Ag tips only at the ends of CdSe nanorods at t = 4 h. **f** HRTEM of Ag tipped CdSe nanorods aligned horizontally revealing the planes corresponding both to CdSe and Ag

1 h stirring of the biphasic mixture which was clearly evidenced in the TEM image, Fig. 1d, and the corresponding STEM image in the inset of the same.

The Ag dots showed a strong preference for migration towards the ends of the CdSe rods on prolonged reaction ($\sim$4 h), ripening to a larger metal tip (4–7 nm) on one or both ends (TEM image, Fig. 1e). The persistence of some unripened dots on the lateral sides of the CdSe nanorods was also evident. HRTEM of a single tipped rod allowed characterisation of the CdSe (002) and Ag (111) lattice spacings at 3.55 and 2.40 A respectively conclusively proving the growth of Ag metal on CdSe nanorods, Fig. 1f. The presence of the semiconductor nanorods in the organic phase (toluene) and the surface attachment of the DMP molecules clearly enabled the selective transfer of Ag^+ from the aqueous phase and its reduction onto the nanorod. Though DMP molecules were not common for reduction of Ag^+ to form Ag nanoparticles, phenolic OH groups had previously been shown to lead to the reduction of Ag^+ in an alkaline medium [31]. Crucially, the attachment of the DMP to nanorods resulted in metal formation on the nanorod structure whereas in solution it capped the Ag nanoparticles forming a stable dispersion. The phenomenon of multiple Ag dots formation and their Oswald ripening to form one larger single tip could be explained in terms of significant lattice mismatch for Ag

and the semiconductor materials used in this study due to a strain relief mechanism [9, 32–34]. The lattice mismatch and associated strain relief had already been reported to grow small islands of noble metals of a critical atom density which ripen into larger islands as the reaction continued. Robinson and co-workers observed similar strain-dependent island formation on CdS nanorods during the partial cation exchange of Cd^{2+} with Ag^{+} [33]. However, as our protocol favoured reduction of the metal under conditions not conducive to Cd ion removal, cation exchange was not expected as confirmed by detailed characterisation.

The UV–Vis spectrum of as synthesized CdSe NRs showed two peaks at 552 and 674 nm (Fig. 2a, curve 1), which were characteristic of the excitonic band transitions [35]. The absorption spectrum of the Ag–CdSe nanorod hybrid retained the peak at 674 nm and showed a peak at 421 nm. The latter corresponded to the surface Plasmon resonance peak of Ag nanoparticles (Fig. 2a, curve 2). The appearance of a surface plasmon peak characteristic of Ag nanoparticles clearly indicated the reduction of Ag^{+} to form Ag nano-dots onto the semiconductor nanoparticles [36, 37]. The PL peak for CdSe nanorods was found to be centred at ~684 nm, after exciting the sample at 400 nm (Fig. 2b, curve 1). The emission was found to be quenched heavily after the formation of Ag–CdSe nanorod hybrid structures (Fig. 2b, curve 2). This kind of quenching of emission peak was probably due to hybrid formation and had previously been reported. It could be explained due to efficient electron transfer from semiconductors to metal nanoparticles [9–11, 38]. The dramatic quenching of emission was suggestive of charge separation at a silver metal–CdSe semiconductor interface. The CdSe–Ag_2Se interface in contrast is an abrupt n–n heterojunction which had a limited effect on the PL intensity as observed in previous studies [39].

The X-ray diffractograms of CdSe nanorods after reaction with $AgNO_3$ revealed the presence of Ag (111), (200) and (220) peaks (Fig. 3a), confirming the presence of fcc Ag with a lattice parameter estimated to be 4.08 A (PCPDF no. 04-0783). It also showed the basic pattern of wurtzite CdSe remained unchanged indicating equally good crystallinity even after the tip formation. The comparatively sharp (002) peak of CdSe indicated the growth of the nanorods

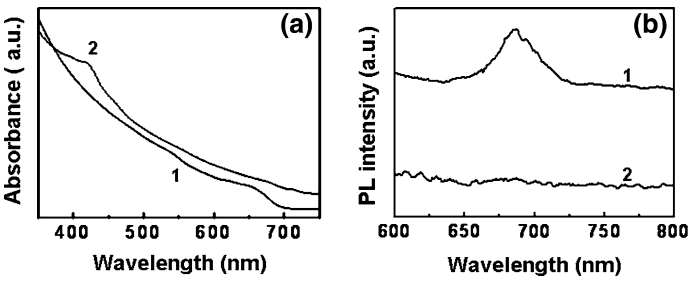

Fig. 2 **a** UV–Vis spectra and **b** photoluminescence spectra of CdSe nanorods, before and after the hybrid formation. In both cases, *curve 1* indicates the as synthesized nanorods whereas *curve 2* corresponds to semiconductor–Ag hybrids

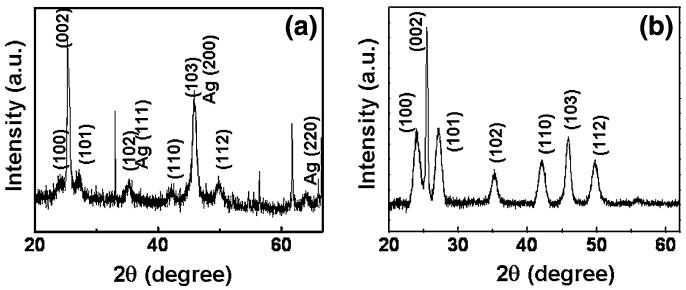

Fig. 3 **a** X-Ray diffractograms of CdSe–Ag hybrids. The peaks for Ag were mentioned in the curve and the rest were matched with wurtzite CdSe. **b** XRD of pristine CdSe nanorods

along this direction which was in exact agreement with the HRTEM in Fig. 1. XRD analysis of pristine CdSe was also performed for comparison which matched well with the wurtzite CdSe (Fig. 3b).

A systematic XPS analysis was carried out on the pristine CdSe nanorods as well as on the hybrid (Fig. 4a–e). In both the cases Cd 3d peak was fitted with two components corresponding to $3d_{5/2}$ and $3d_{3/2}$ at 405.0 and 411.7 eV respectively, Fig. 4a, c. The fitting clearly showed the presence of single species for Cd coming from CdSe. The deconvolution of Se 3d peak showed the presence of two decoupled components at 53.5 and 54.6 eV. (Fig. 4b, d) due to $3d_{5/2}$ and $3d_{3/2}$ which appeared from CdSe. Absence of any extra components in the fitted curve ruled out the probability of the presence of un-reacted Se. The Ag 3d doublet obtained from the hybrids appears at 367.9 and 373.9 eV, with a separation of 6.0 eV and full width at half maximum of 0.9 eV, characteristic of metallic silver [40] (Fig. 4e). However, since the energy differences between the different chemical states of Ag were <0.5 eV, formation of Ag compounds could not be ruled out entirely solely depending on XPS [39]. However, in combination with HRTEM, UV–Vis, and XRD, the characterizations were indicative of metallic Ag tips on rods instead of Ag_2X (X = S, Se) [41] suggesting the phase transfer of Ag^+ ions and their reduction by DMP occurred faster than cation exchange processes [42].

FTIR analyses were also carried out on CdSe rods capped with ligands (Fig. 5) showing the characteristic peaks at 1,463, 1,376, 1,151 and 1,087 cm^{-1} which were related to $–CH_3$ groups of the capping ligand, P = O of alkyl phosphonic acids [43], P = O of TOPO [44] and P–O–H of alkyl phosphonic acids [44] respectively, curve 1, Fig. 5. After modification of the surface with DMP, curve 2, Fig. 5, a new peak at 1,409 cm^{-1} and a broad band at 3,250 cm^{-1} emerged corresponding to –OH in plane bending vibration and stretching vibration respectively of the molecule. Though it was difficult to conclude on the surface ligand composition solely based on these FTIR analyses [45], it was observed that the –OH stretching frequency was damped out after the formation of Ag tips on the particles (Fig. 5, curve 3). This further supported the proposed role of phenolic –OH of DMP in the formation

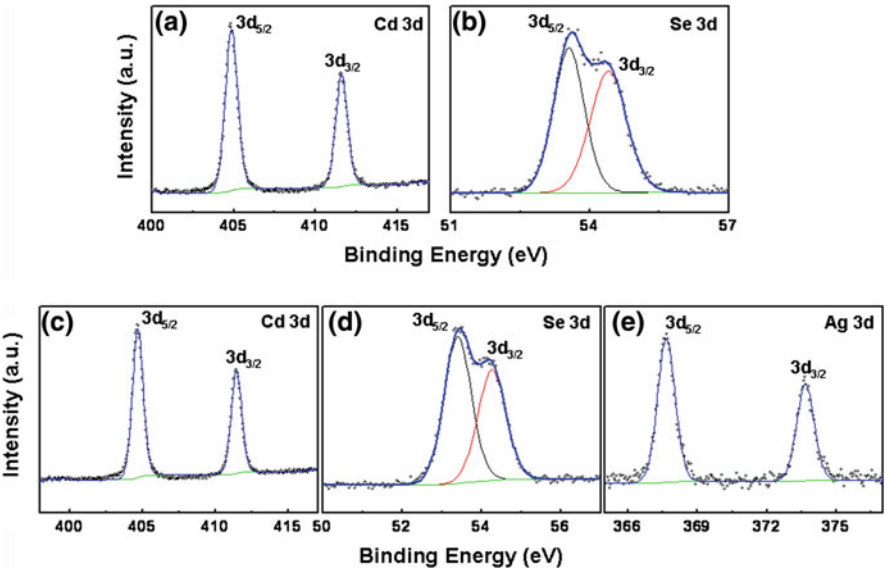

Fig. 4 **a, b** X-Ray photoelectron spectroscopic analysis of Cd 3d, Se 3d from neat CdSe nanorods. **c–e** Same for Cd 3d, Se 3d and Ag 3d from Ag tipped CdSe nanorods

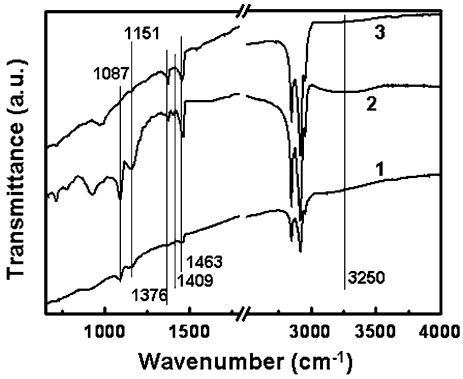

Fig. 5 FTIR analysis of the pristine CdSe rods (*curve 1*), CdSe nanorods after modifying the surface with DMP (*curve 2*) and after the formation of CdSe rod–Ag hybrid (*curve 3*)

of Ag tips on the CdSe rods. It was interesting to note that in the absence of DMP molecules none of the nanorods allowed the growth of any Ag dots which again validated our proposition that DMP played the important roles of phase transfer and reduction of the metal ions site selectively on the surface of the semiconductor materials to synthesize these hybrids.

Through careful control of concentration, Ag-tipped CdSe rods readily organized into close packed vertical assemblies from solution, as observed from TEM and STEM analyses (Fig. 6a and inset). Arrows highlighted the non-assembled

Ag–CdSe rods at the edge of the super lattice. A further magnified TEM image clearly showed the vertically arranged Ag tipped wurtzite rods adopted a hexagonal close packed super-structure with individual rods separated at 1–2 nm by interdigitation of the surfactant ligands, Fig. 6b. The planes corresponding to both CdSe and Ag could be distinguished on the top end of a vertical rod through HRTEM imaging (Fig. 6c). The tipped rods adopted an orthogonal orientation with the CdSe component in contact with the substrate similar to Au-tipped CdSe structures reported by Zhao et al. [17] and O'Sullivan et al. [9, 23]. Brighter contrast due to Ag tips was also clearly visible on vertically aligned CdSe rods under a scanning electron microscope, Fig. 6d. The SEM image of some of the laterally aligned rods is shown in the inset, Fig. 6d.

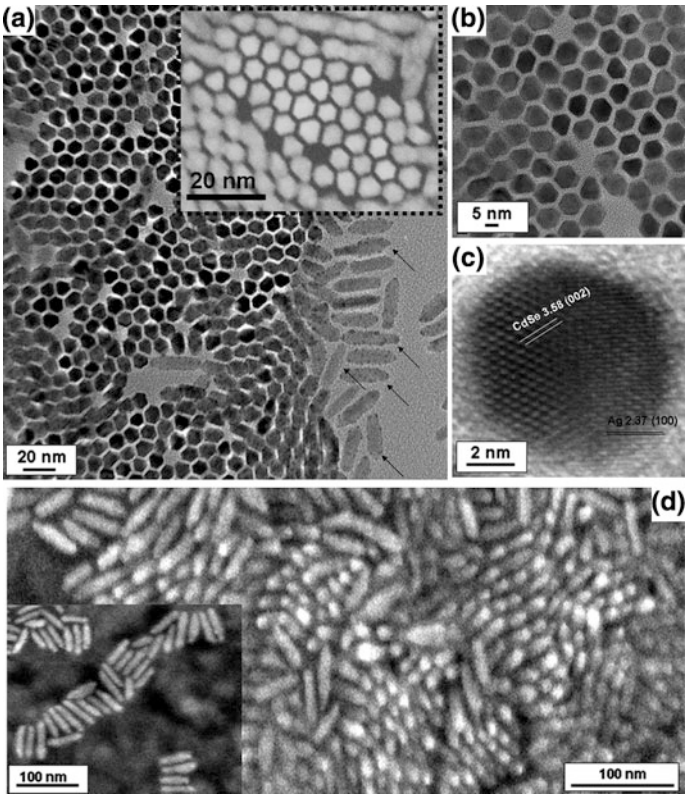

Fig. 6 Vertically assembled Ag-tipped CdSe nanorods at lower **a** and at higher magnification **b**. The STEM image of these assembled hybrids are shown in the inset of (**a**). **c** HRTEM of the vertically aligned hybrid nanorod showing the planes corresponding to both CdSe and Ag. **d** The SEM image of the Ag-tipped CdSe nanorods mainly aligned vertically on the substrate along with few horizontally aligned rods in the inset

4 Conclusion

In summary, we demonstrated a novel synthetic protocol for the formation of Ag noble metal tips on semiconductor nanorods where water soluble metal precursors were transferred to organic media and selectively reduced on nanorods in a single step. This facile route was mediated by an organic ligand (phenolic-OH) which could mediate phase transfer in addition to metal ion reduction at room temperature, thus avoiding the use of costly organometallic precursors and/or toxic organic solvents. The procedure can be extended to a generalized method for different noble metal tipping on semiconductor nanorods through judicious selection of suitable precursors and ligands. The facile hierarchical assembly of the metal tipped nanorods may allow scalable application for bulk devices where nanoscale metal–semiconductor interfaces are required in high density.

Acknowledgments TB acknowledges University of Calcutta for financial support (UGC/1039/Nano Travel Grant) to participate in the conference. The financial supports by Science Foundation Ireland (SFI, Contract No. 06/IN.1/I85 at UL), Institutional funding from INSPIRE are gratefully acknowledged.

Notes and References

1. A.I. Hochbaum, P. Yang, Semiconductor nanowires for energy conversion. Chem. Rev. **110**, 527 (2010)
2. D.V. Talapin, J.-S. Lee, M.V. Kovalenko, E.V. Shevchenko, Prospects of colloidal nanocrystals for electronic and optoelectronic applications. Chem. Rev. **110**, 389 (2010)
3. J. Liqiang, Q. Yichun, W. Baiqi, L. Shudan, J. Baojiang, Y. Libin, F. Wei, F. Honggang, S. Jiazhong, Review of photoluminescence performance of nano-sized semiconductor materials and its relationships with photocatalytic activity. Sol. Energy. Mater. Sol. Cells. **90**, 1773 (2006)
4. R. Costi, A.E. Saunders, E. Elmalem, A. Salant, U. Banin, Visible Light-Induced Charge Retention and Photocatalysis with Hybrid CdS–Au Nano dumbbells. Nano Lett. **8**, 637 (2008)
5. X. Chen, S.S. Mao, Titanium Dioxide nanomaterials: synthesis, properties, modifications and applications. Chem. Rev. **107**, 2891 (2007)
6. D.V. Talapin, I. Mekis, S. Gotzinger, A. Kornowski, O. Benson, H. Weller, CdSe/CdS/ZnS and CdSe/ZnSe/ZnS core−shell − shell nanocrystals. J. Phys. Chem. B **108**, 18826 (2004)
7. C. O'Sullivan, R.D. Gunning, A. Sanyal, C.A. Barrett, H. Geaney, F.R. Laffir, S. Ahmed, K.M. Ryan, Spontaneous room temperature elongation of CdS and Ag2S nanorods via oriented attachment. J. Am. Chem. Soc. **131**, 12250 (2009)
8. S. Ahmed, K.M. Ryan, Centimeter scale assembly of vertically aligned and close packed semiconductor nanorods from solution. Chem. Commun. **42**, 6421 (2009)
9. C. O'Sullivan, S. Ahmed, K.M. Ryan, Gold tip formation on perpendicularly aligned semiconductor nanorods assemblies. J. Mater. Chem. **18**, 5218 (2008)
10. C. O'Sullivan, R.D. Gunning, C.A. Barrett, A. Singh, K.M. Ryan, Size controlled gold tip growth onto II-VI nanorods. J. Mater. Chem. **20**, 7875 (2010)
11. T. Mokari, E. Rothenberg, I. Popov, R. Costi, U. Banin, Selective growth of metal tips onto semiconductor quantum rods and tetrapods. Science **304**, 1787 (2004)

12. T. Mokari, C.G. Sztrum, A. Salant, E. Rabani, U. Banin, Formation of asymmetric one sided metal tipped semiconductor naocrystals dots and rods. Nat. Mater. **4**, 855 (2005)
13. A.E. Saunders, I. Popov, U. Banin, Synthesis of hybrid CdS−Au colloidal nanostructures. J. Phys. Chem. B **110**, 25421 (2006)
14. L. Carbone, S. Kudera, C. Giannini, G. Ciccarella, R. Cingolani, P.D. Cozzoli, L. Manna, Selective reactions on tips of semiconductor nanorods. J. Mater. Chem. **16**, 3952 (2006)
15. W.L. Shi, H. Zeng, Y. Sahoo, T.Y. Ohulchansky, Y. Ding, Z.L. Wang, M. Swihart, P.N. Prasad, A general approach to binary and ternary hybrid nanocrystals. Nano Lett. **6**, 875 (2006)
16. D.V. Talapin, E.V. Shevchenko, C.B. Murray, A. Kornowski, S. Forster, H. Weller, CdSe and CdSe/CdS nanorod solids. J. Am. Chem. Soc. **126**, 12984 (2004)
17. N. Zhao, K. Liu, J. Greener, Z. Nie, E. Kumacheva, Close-packed super lattices of side-by-side assembled Au-CdSe nanorods. Nano Lett. **9**, 3077 (2009)
18. A. Salant, E.A. Sadovsky, U. Banin, Directed self-assembly of gold-tipped CdSe nanorods. J. Am. Chem. Soc. **128**, 10006 (2006)
19. C.A.J. Lin, T.Y. Yang, C.H. Lee, S.H. Huang, R.A. Sperling, M. Zanella, J.K. Li, J.L. Shen, H.H. Wang, H.I. Yeh, W.J. Parak, W.H. Chang, Synthesis, characterization, and bioconjugation of fluorescent gold nanoclusters toward biological labeling applications. ACS Nano **3**, 395 (2009)
20. V.R. Reddy, N.R. Reddy, C.-J. Choi, Electrical and structural properties of low-resistance Pt/Ag/Au ohmic contacts to p-type GaN. Solid-State Electron. **49**, 1213 (2005)
21. M.T. Sheldon, P.-E. Trudeau, T. Mokari, L.-W. Wang, A.P. Alivisatos, Enhanced semiconductor nanocrystal conductance via solution grown contacts. Nano Lett. **9**, 3676 (2009)
22. K.T. Yong, Y. Sahoo, K.R. Choudhury, M.T. Swihart, J.R. Minter, P.N. Prasad, Shape control of PbSe nanocrystals using noble metal seed particles. Nano Lett. **6**, 709 (2006)
23. C. O'Sullivan, S. Crilly, F.R. Laffir, A. Singh, E. Magner, K.M. Ryan, Protein immobilization on perpendicularly aligned gold tipped nanorods assemblies. Chem. Commun. **47**, 2655 (2011)
24. S.E. Habas, P. Yang, T. Mokari, Selective growth of metal and binary metal tips on CdS nanorods. J. Am. Chem. Soc. **130**, 3294 (2008)
25. B.D. Yuhas, S.E. Habas, S.C. Fakra, T. Mokari, Probing compositional variation within hybrid nanostructures. ACS Nano **3**, 3369 (2009)
26. L.-Y. Fan, S.-H. Yu, ZnO@Co hybrid nanotube arrays growth from electrochemical deposition: structural, optical, photocatalytic and magnetic properties. Phys. Chem. Chem. Phys. **11**, 3710 (2009)
27. J. Maynadie, A. Salant, A. Falqui, M. Respaud, E. Shaviv, U. Banin, K. Soulantica, B. Chaudret, Cobalt growth on tips of CdSe nanorods. Angew. Chem. Int. Ed. **48**, 1814 (2009)
28. E. Elmalem, A.E. Saunders, R. Costi, A. Salant, U. Banin, Growth of photocatalytic CdSe-Pt nanorods and nanonets. Adv. Mater. **20**, 4312 (2008)
29. A. Singh, R.D. Gunning, A. Sanyal, K.M. Ryan, Directing semiconductor nanorods assembly into 1D or 2D super crystals by altering the surface charge. Chem. Commun. **46**, 7193 (2010)
30. I. Gur, N.A. Fromer, M.L. Geier, A.P. Alivisatos, Air-stable all-inorganic nanocrystal solar cells processed from solution. Science **310**, 462 (2005)
31. P.R. Selvakannan, A. Swami, D. Srisathiyanarayanan, P.S. Shirude, R. Pasricha, A.B. Mandale, M. Sastry, Synthesis of aqueous Au Core−Ag shell nanoparticles using tyrosine as a pH-dependent reducing agent and assembling phase-transferred silver nanoparticles at the air−water interface. Langmuir **20**, 7825 (2004)
32. B. Muller, L.P. Nedelmann, B. Fischer, H. Brune, J.V. Barth, K. Kern, D. Erdos, J. Wollschlager, Strain relief via island ramification in sub monolayer herero epitaxy. Surf. Rev. Lett. **5**, 769 (1998)
33. R.D. Robinson, B. Sadtler, D.O. Demchenko, C.K. Erdonmez, L.W. Wang, A.P. Alivisatos, Spontaneous superlattice formation in nanorods through partial cation exchange. Science **317**, 355 (2007)

34. D.H. Son, S.M. Hughes, Y. Yin, A.P. Alivisatos, Cation Exchange Reactions in Ionic Nanocrystals. Science **306**, 1009 (2004)
35. G. Ramalingam, N. Melikechi, P. DennisChristy, S. Selvakumar, P. Sagayaraj, Structural and optical property studies of CdSe crystalline nanorods synthesized by a solvothermal method. J. Cryst. Growth **311**, 3138 (2009)
36. J.A. Creighton, D.G. Eadon, Ultraviolet–visible absorption spectra of the colloidal metallic elements. J. Chem. Soc., Faraday Trans. **87**, 3881 (1991)
37. A. Kumar, V. Chaudhary, Optical and photophysical properties of Ag/CdS nanocomposites—An analysis of relaxation kinetics of the charge carriers. J. Photochem. Photobiol. A **189**, 272 (2007)
38. Y.P. Hsieh, C.T. Liang, Y.F. Chen, C.W. Lai, P.T. Chou, Mechanism of giant enhancement of light emission from Au/CdSe nanocomposites. Nanotechnology **18**, 415707 (2007)
39. L.K. Leung, N.J. Komplin, A.B. Ellis, N. Tabatabaie, Photoluminescence studies of silver-exchanged cadmium selenide crystals: Modification of a chemical sensor for aniline derivatives by heterojunction formation. J. Phys. Chem. **95**, 5918 (1991)
40. NIST X-ray Photoelectron Spectroscopy Database, Version 3.5, http://srdata.nist.gov/xps/
41. J. Yang, E. Sargent, S. Kelley, J. Y. Ying, A general phase-transfer protocol for metal ions and its application in nanocrystal synthesis. Nat. Mater. **8**, 683 (2009)
42. S. Chakrabortty, J.A. Yang, Y.M. Tan, N. Mishra, Y. Chan, Asymmetric Dumbbells from Selective Deposition of Metals on Seeded Semiconductor Nanorods. Angew. Chem. **122**, 2950 (2010)
43. R. Luschtinetz, G. Seifert, E. Jaehne, H. J. P. Adler, Infrared Spectra of Alkylphosphonic Acid Bound to Aluminium Surfaces. Macromol. Symp. **254**, 248 (2007)
44. P.K. Sahoo, S.S.K. Kamal, M. Premkumar, T.J. Kumar, B. Sreedhar, A.K. Singh, S.K. Srivastava, K.C. Sekhar, Synthesis of tungsten nanoparticles by solvothermal decomposition of tungsten hexacarbonyl. Int. J. Refract. Met. Hard Mater. **27**, 784 (2009)
45. A.J. Morris-Cohen, M.D. Donakowski, K.E. Knowles, E.A. Weiss, The Effect of a Common Purification Procedure on the Chemical Composition of the Surfaces of CdSe Quantum Dots Synthesized with Trioctylphosphine Oxide. J. Phys. Chem. C **114**, 897 (2010)